Chemical Physics Letters 754 (2020) 137639

Contents lists available at ScienceDirect

Chemical Physics Letters

journal homepage: www.elsevier.com/locate/cplett

Research paper

Structural, optical and photocatalytic properties of ZnS spherical/flake nanostructures by sugar-assisted hydrothermal process

J. Gajendiran[a,*], S. Gnanam[b,*], V. Vijaya Kumar[c], K. Ramachandran[d], J. Ramana Ramya[e], S. Gokul Raj[f], N. Sivakumar[g]

[a] Department of Physics, Vel Tech Rangarajan Dr.Sagunthala R&D Institute of Science and Technology, Avadi, Chennai 600 062, India
[b] Department of Physics, School of Basic Sciences, Vels Institute of Science, Technology & Advanced Studies (VISTAS), Pallavaram, Chennai 600 117, Tamilnadu, India
[c] Department of Chemistry, Anna University, CEG Campus, Chennai 600 025, Tamil Nadu, India
[d] Department of Physics, SRMIST, Vadapalani Campus, Chennai 600026, India
[e] National Center for Nanoscience and Nanotechnology, University of Madras, Chennai 600025, India
[f] Department of Physics, C.Kandaswami Naidu College for Men, Annanagar, Chennai 600102, Tamilnadu, India
[g] Crystal Growth Centre, Anna University, Chennai 600025, India

HIGHLIGHTS

- Spherical and flake/spherical shaped ZnS nanostructures were prepared by the hydrothermal method.
- The sphalerite and wurtzite crystal structure of the ZnS samples has been confirmed in the XRD analysis.
- In the SEM and TEM analysis, the flake/spherical particles of the S-ZS samples were observed.
- Studies of UV and FL showed better optical absorption and luminescence behavior of the S-ZS sample.
- The photocatalytic degradation of the MO dye using ZS and S-ZS samples has been studied.

ARTICLE INFO

Keywords:
Semiconductor
Metal sulfide
Nanostructure
Hyrothermal process
Optical properties
Photocatalytic properties

ABSTRACT

The mixed morphology of semiconducting metal sulfide nanostructured materials has been the hotspot of research. In this paper, we have reported the sugar assisted hydrothermal method, applied to prepare spherical/flake surface morphology of ZnS nanostructures. The crystal structure, surface morphology, light absorption, energy gap, emission peak, surface defects and photocatalytic properties of ZnS materials have been examined through the XRD, SEM, TEM, UV–visible, FL and photocatalytic studies. A solution of methyl orange dye is mixed with prepared ZnS samples under the illumination of UV-light; the photocatalytic degradation absorption, and efficiency have been estimated from the optical spectra of this mixtures.

1. Introduction

In the past few years, the mixed morphology of semiconductor based metal sulfide materials has been investigated using the UV–visible and photoluminescence (PL) spectra for optical and emission behavior analysis [1–9]. On the basis of the above literature, excellent optical properties have been found in the mixed morphology of the metal sulfide material compared to the homogeneity of the surface morphology of the material. For example, CdS, CuS and SnS_2 materials have a narrow energy gap, and an absorption edge in the visible portion and are toxic [4–9]. Among the metal sulfides, ZnS has some unique properties, such as broad light absorption in the ultraviolet portion, wide energy gap and non-toxicity. Therefore, the above properties of ZnS have been used mainly in optical, electronic, photoconductive, and photovoltaic devices and for photocatalysts [1–3,10–12].

ZnS material changes in particle size, shape, optical energy gap, emission intensity and surface defects, depending on its cubic and hexagonal crystal structure [13,14]. This crystal structure could be produced under the influence of ligands, solvents, reaction temperatures and time intervals, doping and surface modifier, ratio of zinc salt/

* Corresponding authors at: Department of Physics, Vel Tech Rangarajan Dr.Sagunthala R&D Institute of Science and Technology, Avadi, Chennai 600 062, India (J. Gajendiran). Department of Physics, School of Basic Sciences, Vels Institute of Science, Technology & Advanced Studies (VISTAS), Pallavaram, Chennai 600 117, Tamilnadu, India (S. Gnanam).
E-mail addresses: gaja.nanotech@gmail.com (J. Gajendiran), gnanam.nanoscience@gmail.com (S. Gnanam).

https://doi.org/10.1016/j.cplett.2020.137639
Received 4 May 2020; Received in revised form 15 May 2020; Accepted 21 May 2020
Available online 23 May 2020

sulfur source, etc. [1,2,13–17]. Far less research has been done to study the mixed morphology of the zinc sulphide material's structural, optical, photoluminescent and photocatalytic properties.

2. Experimentals

2.1. Synthesis of ZnS nanoparticles by the hydrothermal method

1.8348 g of dicarbomethoxyzinc dehydrate solid (Zn $(CH_3CO_2)_2{\cdot}2H_2O$) and 1 g of sugar were dispersed in 80 mL of double distilled water with continuous stirring and 0.7612 g of thiocarbamide (CH_4N_2S) was applied in the same beaker for a further 30 min of stirring. After, the release of the S source from thiocarbamide and zinc from dicarbomethoxyzinc, the production of acetic acid and sugar molecules reacting with water occurred due to hydrolysis and dissociation of ions under constant magnetic stirring. The above reaction mixture was transferred to a Teflon stainless steel autoclave and tightly closed. Then, the autoclave was held at a temperature of 180 °C for 24 h at a ramping rate of 5 °C/min. During this process, by-products like acetic acid, and amine can be removed and only ZnS formed from the Zn-sulfur precursor complex. The resulting products were washed two times in a liquid medium (double distilled water) accompanied by ethyl alcohol. This was for the removal of impurities on the surface of the ZnS product. The obtained wet black powder was dried for 6 hrs in a hot air vacuum at 60 °C and stored sugar assisted ZnS powder (S-ZS sample) in desiccated soil. The reason for driying is to remove the wetness from the powder. Likewise, ZnS powder (ZS sample) without adding any sugar content was also prepared for comparison purposes under similar conditions.

2.2. Characterization

The synthesized ZnS samples was performed on the XPERTPRO XRD diffractometer using the CuK_α radiation and applying a wavelength of 1.5414 Å at a scanning rate of 0.02 to determine the crystalline phase structure. S-3400-SEM microscope tested the internal surface morphology of the prepared samples. H-800 -TEM (Hitachi, Japan) found the particle size and shape of the prepared ZnS samples. Jasco V-760 UV–visible spectromete recorded the spectral wavelength portion of 200–600 nm for determining the optical band gap values of the ZnS samples. The emission behavior has been tested on the Fluorescence spectrometer (model EP-8300) in the spectral wavelength range between 400 and 700 nm.

2.3. Photocatalytic experiement

The photocatalytic activity was found by mixing the degradation of the MO dye/prepared ZnS solution, using the Heber-Multilamp photoreactor. Hitachi U-2000 double beam UV–vis spectrophotometer. 50 mg of ZnS samples and 5.0×10^{-4} M concentration of MO dye were taken for the photocatalytic experiment. The degradation of MO dye/prepared ZnS samples solution was collected at different irradiation time intervals and the solution has been tested for the optical absorption using the UV–visible spectra.

3. Results and discussion

In Fig. 1 (a &b), the crystalline phase of the absence and presence of sugar assisted ZnS samples was analyzed in the range of 2θ between 10° and 70°. Both the XRD patterns had different crystalline structures, such as sphalerite (Fig. 1a) and wurtzite (Fig. 1b) [14,18]. The reflection peaks of the prepared ZnS samples were noticed at different scattering angles in the XRD pattern, depending on the lack or presence of the sugar content in the ZnS complex. In addition, Fig. 1a showed a crystalline nature, while the addition of a sugar-assisted ZnS sample is a high crystalline nature.

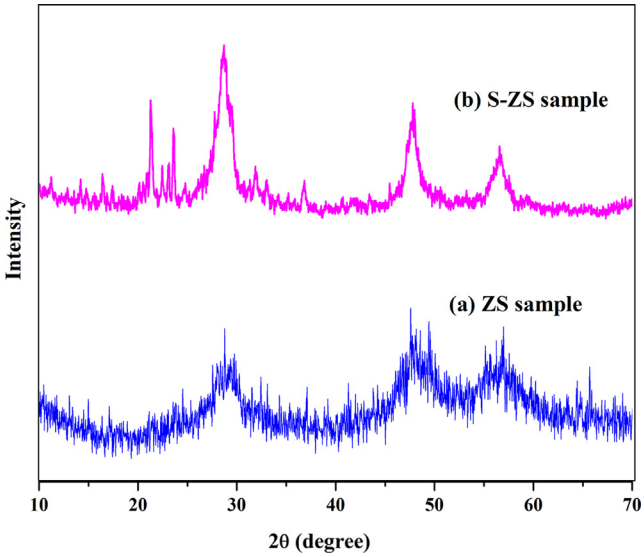

Fig. 1. XRD pattern of (a) ZS and (b) S-ZS samples.

The SEM pictures of the prepared ZS and S-ZS samples are shown in Fig. 2(a&b). The ZS sample revealed irregular spherical shaped particles, while the S-ZS sample showed a mixed morphology such as spherical with flake-like particles. Based on the above-mentioned SEM studies, we concluded that the adding of sugar content is vital to the formation of a mixed particle morphology in the ZnS sample. Fig. 2c displayed the TEM picture of the S-ZS sample. It clearly showed the spherical with flake-like particle morphology, which were well supported by the SEM studies. Moreover, the particle size of the S-ZS sample was measured in the range of 10–35 nm in the TEM picture.

Strong absorption peaks were noticed in the wavelength of 319 and 317 nm for the ZS and S-ZS samples in the ultraviolet portion, as depicted in Fig. 3a(a & b). This suggested that the prepared ZS and S-ZS samples are materials having a broad band gap. We could estimate the energy gap in the prepared samples directly, if a sharp light absorption peak is detected in the UV–visible spectra. The energy band gap values were then directly estimated by the energy gap equation $E_g = hc/\lambda_{abs}$ (where, λ_{abs}- absorption edge, h-Planck's constant, and c-velocity of light) [18]. The energy gap was computed around 3.88 and 3.91 eV for the ZS and S-ZS samples. The higher energy gap values for the ZS and S-ZS samples are obtained as compared to the bulk energy gap value of the ZnS material (3.72 eV) [15]. This indicated the nano-sized impact on the prepared samples. The prepared samples can also be used for optical and electronics applications.

Strong visible emission bands were detected in the wavelength of 590 nm in both the fluorescence (FL) spectra of the ZnS samples (Fig. 3b). The presence of a visible emission band indicated the sulfur vacancy defects in both the prepared ZnS samples. The S-ZS sample has less sulfur vacancy defects (ie less emission intensity) compared to the ZS sample in the FL spectra. Kaur et al. [1], Gao et al. [14], Amaranatha Reddy et al. [16], Sathiyaraj et al. [19] and Sarkar et al. [20] have investigated the high visible emission peaks of ZnS content comparable to the PL results obtained.

In order to measure the photocataltyic degradation efficiency, a photocatalytic experiment was performed by mixing the MO organic dye solution and the ZS and S-ZS samples were prepared as photocatalysts under continuous UV-light radiation at various time intervals (Fig. 3c). A variety of degradation solutions were then collected at intervals and the UV–visible spectra were taken. The obtained optical spectra of the degradation solution samples at different time intervals and their absorbance values are measured in the final concentration (C) of degradation and the initial concentration (C_o) of degradation. After that, the time interval between the MO degradation and irradiation was

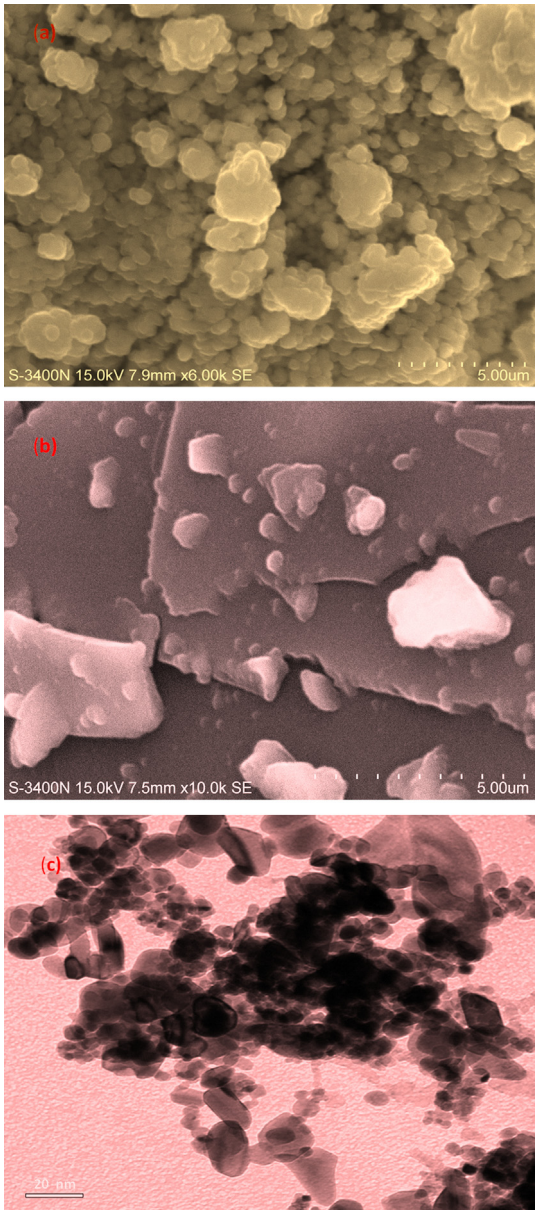

Fig. 2. SEM pictures of (a) ZS, (b) S-ZS samples and (c) TEM picture of S-ZS nanostructures.

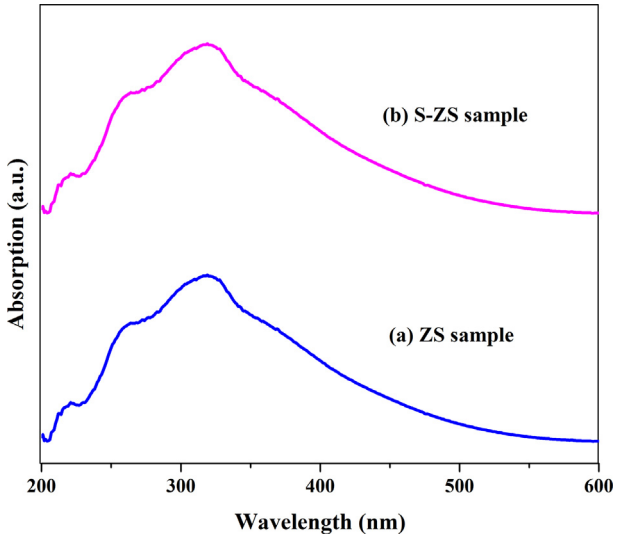

Fig. 3a. UV–visible spectra of (a) ZS and (b) S-ZS nanostructures samples.

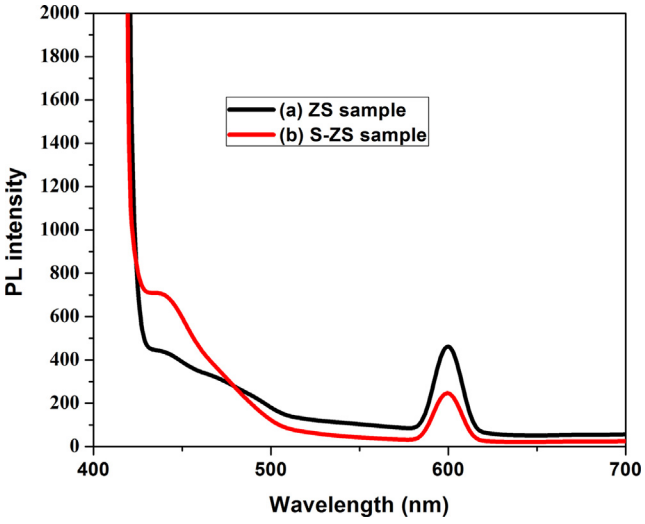

Fig. 3b. FL spectra of (a) ZS and S-ZS nanostructures samples.

plotted. The photocataltyic degradation efficiency values are estimated to be around 51.7 and 84% of the ZS and S-ZS samples at the light irradiation time intervals of 150 min. The decreasing absorbance of the MO dye in the optical spectra with respect to increasing irradiation time intervals, indicated the removal of the MO dye from the solution. This degradation happened due to two reasons: (i) continuously applied light radiation and (ii) the prepared samples acting as a photocatalyst. When light radiation is used on the ZnS photocatalyst/MO dye solution, ZnS materials are absorbed by electromagnetic radiation (photon) to generate the electron-hole pair and release an electron from the ZnS in the valence band (V.B). The photogenerated electron has now been moved to the ZnS conduction band (C.B). The conduction electron interacts with the oxygen molecule absorbed on the surface of the ZnS to create super oxide anion free radicals ($^{\cdot}O_2^-$). The holes generated in the V.B react with the surface hydroxyl group to produce free radicals of the hydroxyl group ($^{\cdot}OH^-$). Subsequently, super oxide radicals and free radicals of hydroxyl react with the absorbed MO dye/ZnS aqueous soluion to form hydrogen peroxides (H_2O_2). These hydrogen peroxides could degrade the MO dye to produce minerals and remove gases. The most popular commercial TiO_2 named by Degussa P25 TiO_2 (P-TiO_2), containing around 85% anatase and 15% rutile, usually exhibits high photocatalytic activity. However, P-25 TiO_2 exhibits two crystal structures like anatase and rutile [21,22]. Structural stability is one of the factors that enhances the photocatalytic efficiency. In this present work, we reported the photocatalytic activity of 84% obtained for the S-ZS sample with a single crystal structure.

The kinetics of photocatalytic degradation was tested using the pseudo-first order formula given below:

$$-\ln C/C_0 = K.\ t \quad (1)$$

Where, k-reaction rate constant. We can find out the rate constant with the help of the irradiation time (min) on the x-axis and –ln C/C_0 on the y-axis using the linear fit curve as shown in Fig. 3c (d). The reaction rate constant was found to be 0.00524 and 0.0114/min for the ZS and S-ZS samples. Based on the above rate constant results, we can conclude that the S-ZS sample revealed greater degradation rate constant than the ZS sample. In addition, we found the R-square values to be 0.969 and 0.976 for the ZS and S-ZS samples.

4. Conclusions

In this work, we prepared irregular spherical and flake/spherical

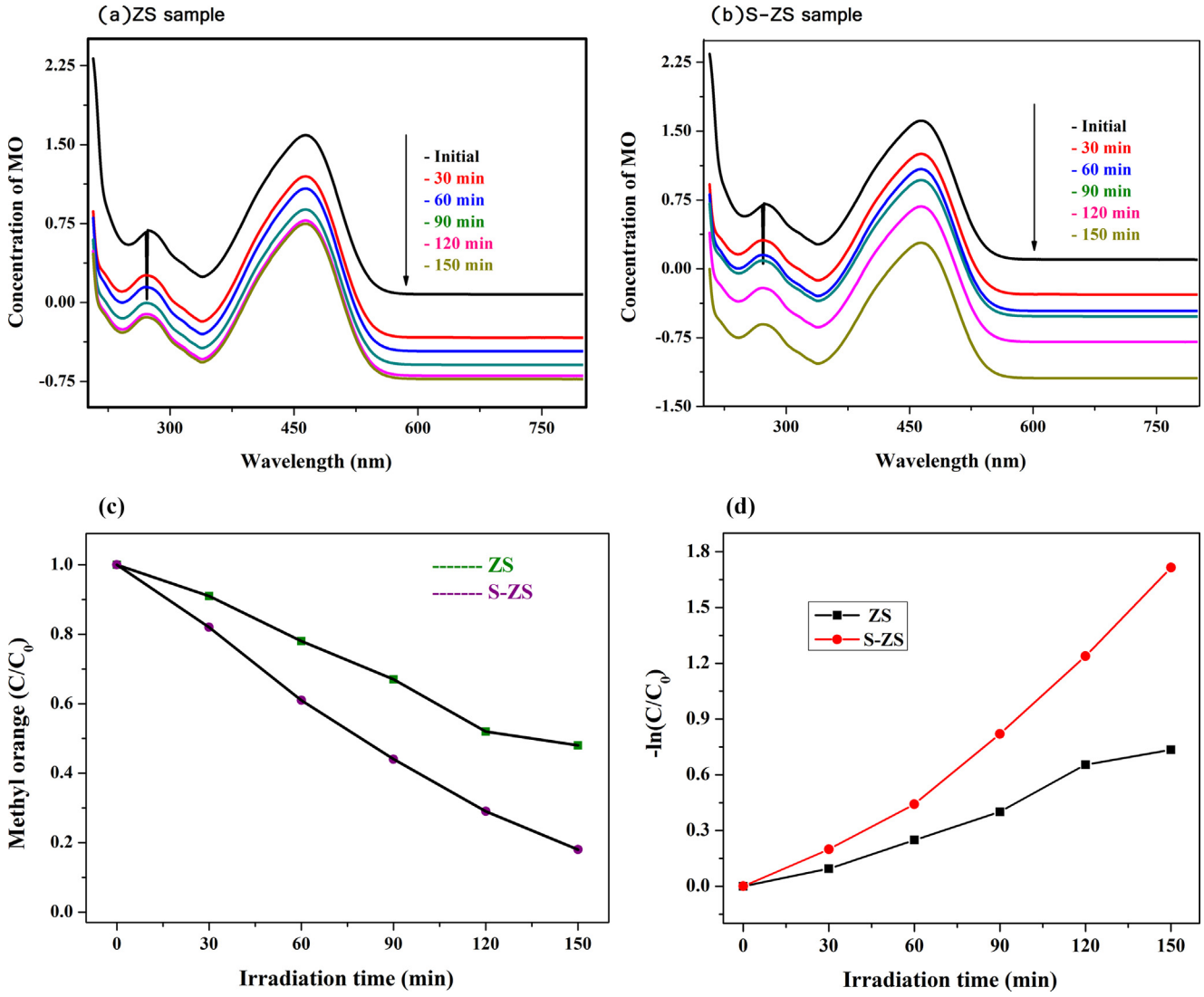

Fig. 3c. (a) UV–visible spectra of degradation of MO dye/ZS sample, (b) degradation of MO dye/S-ZS sample and (c) degradation of MO dye/ZnS samples vs irradiation time and (d) $-\ln C/C_0$ vs irradiation time plots.

morphology of the ZnS microstructure using the hydrothermal method. We observed distinguishing crystal phases such as sphalerite and wurtzite structures in the XRD pattern for the absence and presence of ZnS samples supported by sugar. A variation of the particle surface morphology of the ZnS microstructure was observed in the micrograph due to the addition of sugar content to the ZnS precursor complex. We concluded that, in the UV and FL studies, the sugar assisted ZnS sample had better optical (decreasing optical band) and luminescence (less surface defect i.e. decreasing sulfur vacancy and emission intensity) and photocatalytic properties compared to the non-sugar-assisted sample.

CRediT authorship contribution statement

J. Gajendiran: Methodology, Investigation, Writing - review & editing. **S. Gnanam:** Investigation, Writing - review & editing, Conceptualization. **V. Vijaya Kumar:** Methodology. **K. Ramachandran:** . **J. Ramana Ramya:** Formal analysis. **S. Gokul Raj:** . **N. Sivakumar:** Formal analysis.

Declaration of Competing Interest

The authors declare that they have no known competing financial interests or personal relationships that could have appeared to influence the work reported in this paper.

Appendix A. Supplementary material

Supplementary data to this article can be found online at https://doi.org/10.1016/j.cplett.2020.137639.

References

[1] B. Kaur, K. Singh, A.K. Malik, Effect of ligands on crystallography, morphology and photo-catalytic ability of ZnS nanostructures, Dyes. Pigm. 142 (2017) 153–160.
[2] R. Mendil, Z.B. Ayadi, K. Djessas, Effect of solvent medium on the structural, morphological and optical properties of ZnS nanoparticles synthesized by sol-vothermal route, J. Alloys. Comp. 678 (2016) 87–92.
[3] H. Wu, Q. Wang, Y. Yao, C. Qian, X. Zhang, X. Wei, Microwave-assisted synthesis and photocatalytic properties of carbon nanotube/zinc sulfide hetereostructures, J. Phys. Chem. C. 112 (2008) 43.
[4] X. Zhou, J. Huang, H. Zhang, H. Sun, W. Tu, Controlled synthesis of CdS nano-particles and their surface loading with MoS_2 for hydrogen evolution under visible light, Int. J. Hydrogen. Energy. 41 (2016) 14758–14767.
[5] J. Zhu, M. Zhou, J. Xu, X. Liao, Preparation of CdS and ZnS nanoparticles using microwave Irradiation, Mater. Lett. 47 (2001) 25–29.
[6] R. Sing, B. Pal, Fine-tuning the photoluminescence and photocatalytic properties of CdS nanorods of varying dimensions, Mater. Res. Bullet. 48 (2013) 1403–1410.
[7] F. Mammeri, A. Ballarin, M. Giraud, G. Brustin, Photoluminescence properties of new quantum dot nanoparticles/carbon nanotubes hybrid structures, Colloids. Surf A: Physicochem. Eng. Aspects 439 (2013) 138–144.

[8] A. Putta Rangappa, D. Praveen Kumar, M. Gopannagari, D. Amaranaatha Reddy, Y. Hong, Y. Kim, et al., Highly efficient hydrogen generation in water using 1 DS CdS nanorods integrated with 2D SnS_2 nanosheets under solar light irradiation, Appl. Surf. Sci. 50 (2020) 144803.
[9] R. Zeinodin, F.J. Sheini, In doped CdS nanostructures: ultrasonic synthesis, physics properties, and enhanced photocatalytic behavior, Physica B: Conden. Matter. 570 (2019) 148–156.
[10] C. Zhou, Q. Wang, C. Zhou, Photocatalytic degradation of antibiotics by molecular assembly porous carbon nitride: Activity studies and artificial neural networks modeling, Chem. Phy. Lett. 750 (2020) 137479.
[11] C. Zhou, Z. Zeng, G. Zeng, D. Huang, R. Xiao, M. Cheng, et al., Visible-light-driven photocatalytic degradation of sulfamethazine by surface engineering of carbon nitride:properties, degradation pathway and mechanisms, J. Hazard. Mater. 380 (2019) 120815.
[12] C. Zhou, G. Zeng, D. Huang, Y. Luo, M. Cheng, Y. Liu, et al., Distorted polymeric carbon nitride via carriers transfer bridges with superior photocatalytic activity for organic pollutants oxidation and hydrogen production under visible light, J. Hazard. Mater. 386 (2020) 121947.
[13] V. Sabaghi, F. Davar, Z. Fereshteh, ZnS nanoparticles prepared via simple reflux and hydrothermal method: optical and photocatalytic properties, Ceram. Int. 44 (2018) 7545–7556.
[14] W. Gao, M. Cao, W. Xiao, F. Lei, J. Huang, Y. Sun, et al., Effects of reaction conditions on the structural, morphological and optical properties of solvothermal synthesized ZnS nanostructures, Mater. Sci. Semiconduct. Proces. 56 (2016) 349–356.
[15] Y. Wang, Q. Ma, H. Jia, J. Kong, Controllable synthesis, characterization of ZnS nanostructured spheres, J. Mater. Sci. Mater. Electron. 27 (2016) 7167–7173.
[16] D. Amaranatha Reddy, C. Liu, R.P. Vijayalakshmi, B.K. Reddy, Effect of Al doping on the structural, optical and photoluminescence properties of ZnS nanoparticles, J. Alloys. Comp. 582 (2014) 257–264.
[17] B. Poornaprakash, U. Chalapathi, S.V. Youngsuk Suh, M. Prabhakar Vattikuti, Siva Pratap Reddy, Si-Hyun Park, Terbium-doped ZnS quantum dots: Structural, morphological, optical, photoluminescence, and photocatalytic properties, Ceram. Int. 44 (2018) 11724–11729.
[18] Q. Wei, M. Yin, Y. Yao, Synthesis of sphere-like ZnS architectures via a solvothermal method and their visible-light catalytic properties, J. Mater. Sci. Mater. Electronics. 28 (2017) 17827–17832.
[19] E. Sathiyaraj, S. Thirumaran, Structural, morphological and optical properties of iron sulfide, cobalt sulfide, copper sulfide, zinc sulfide and copper-iron sulfide nanoparticles synthesized from single source precursor, Chem. Phy. Lett. 739 (2020) 1136972.
[20] R. Sarkar, C.S. Tiwary, P. Kumbhakar, A.K. Mitra, Enhanced visible light emission from Co^{2+} doped ZnS nanoparticles, Physica B. 404 (2009) 3855–3858.
[21] X. Qin, L. Jing, G. Tian, Y. Qu, Y. Feng, Enhanced photocatalytic activity for degrading Rhodamine B solution of commercial Degussa P25 TiO_2 and its mechanisms, J. Hazard. Mater. 172 (2009) 1168–1174.
[22] J. Wen, J. Xie, X. Chen, X. Li, A review on g-C_3N_4-based photocatalysts, Appl. Surf. Sci. 391 (2017) 72–123.